DOI: 10.61782/fa.2025.0624

FORUM ACUSTICUM
EURONOISE 2025

# NONLINEAR BEHAVIOR OF CONDENSER MICROPHONES: ANALYTICAL MODELING AND EXPERIMENTAL VALIDATION

**Jan Plaček**[1] **Petr Honzík**[1*]
[1] Department of Radioelectronics, Faculty of Electrical Engineering,
Czech Technical University in Prague, Technická 2, 166 27 Praha, Czech Republic

## ABSTRACT

This study investigates the nonlinear behavior of condenser microphones, with a focus on nonlinear capacitance as the primary source of nonlinearity. An experimental transducer was developed, consisting of a circular membrane and a fixed electrode with a central hole leading to a backing cavity. A linear analytical model for membrane displacement was derived using a multimodal approach, while a nonlinear model from the literature was used to relate the membrane displacement to the output voltage of the microphone. Experimental measurements of the nonlinear output of the transducer were conducted. A harmonic correction method from the literature was used to linearize the acoustic pressure incident on the transducer's membrane. These measurements were compared with theoretical predictions. The dependence of the first, second, and third harmonics of the output voltage on the input acoustic pressure level was analyzed. The results show good agreement between theoretical predictions and experimental data, particularly for the first and second harmonics, demonstrating the effectiveness of the proposed model in capturing the nonlinear characteristics of condenser microphones.

**Keywords:** *nonlinear behavior, condenser microphones, analytical modeling, harmonic correction, experimental validation*

**Corresponding author*: honzikp@fel.cvut.cz.


## 1. INTRODUCTION

Condenser microphones offer several advantages, including a flat frequency response, low inherent noise, and relatively high sensitivity. Like many electroacoustic transducers, they exhibit a certain level of nonlinear distortion [1]. Among the various sources of nonlinearity, the nonlinear variation of capacitance is widely recognized as the dominant contributor [2]. This nonlinear distortion can be both measured [3, 4] and, to some extent, reduced [5, 6].

In this paper, we first present an analytical model of an experimental condenser microphone composed of a circular membrane and a fixed electrode with a central hole leading to a backing cavity. A linear formulation is used to determine the membrane displacement, which is then applied to compute the nonlinear output voltage of the microphone. The experimental device is subsequently described, along with a measurement setup based on recent techniques for nonlinear characterization and signal correction [4, 7]. Finally, the measured results are presented and compared with theoretical predictions to assess the accuracy and limitations of the model.

## 2. ANALYTICAL MODEL

This section presents an analytical model of the electrostatic (condenser) microphone, which consists of a circular membrane of radius $R$, separated by an air gap of thickness $h_g$ from a fixed electrode of thickness $l_h$. The electrode contains a central hole of radius $R_h$, which opens into a backing cavity with volume $V_c$, as illustrated in Figure 1.

### 2.1 Nonlinear ouput voltage

First, the model of the microphone output voltage incorporating nonlinearities due to the nonlinear variation of

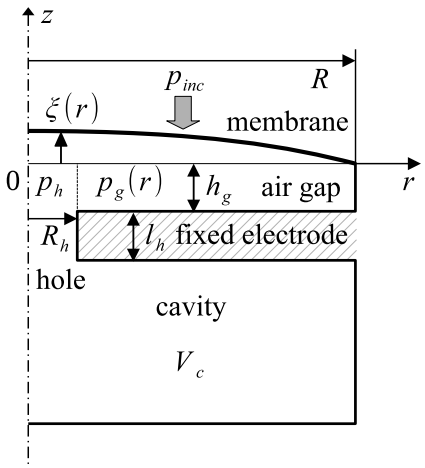


**Figure 1**. Axisymmetric schematic cross-sectional view of the transducer.

capacitance is summarized from [4]. Since the polarization voltage $U_0$ is applied to the fixed electrode through a high-value polarization resistor (on the order of GΩ), the charge variation is negligible, and the output voltage can be expressed as

$$u = -U_0 \frac{\mathrm{d}C}{C}. \tag{1}$$

Assuming that the time-dependent capacitance is given by

$$C(t) = C_p + \frac{\varepsilon_0 S}{h_g + \tilde{\xi}(t)} = C_p + C_0 \frac{1}{1 + \frac{\tilde{\xi}(t)}{h_g}}, \tag{2}$$

where $\tilde{\xi}(t)$ denotes the spatial average of the membrane displacement over the active area of the fixed electrode, the capacitance can be expressed as the sum of the parasitic capacitance $C_p$, transducer's static capacitance $C_0$ and a time-varying component $\mathrm{d}C(t)$. Applying a Taylor series expansion, the output voltage (1) can be written as

$$u(t) = U_0 \frac{C_0}{C_p + C_0} \left( \frac{\tilde{\xi}(t)}{h_g} - \left( \frac{\tilde{\xi}(t)}{h_g} \right)^2 + \right. \\ \left. + \left( \frac{\tilde{\xi}(t)}{h_g} \right)^3 - \dots \right) \tag{3}$$

The nonlinearities in the output voltage are thus clearly apparent.

### 2.2 Equations governing the displacement of the membrane

The membrane displacement $\xi$, required for evaluating the output voltage in (3), is governed by the following wave equation [8–10]

$$T(\Delta_r + K^2)\xi(r) = p_{inc} - p(r), \tag{4}$$

where $T$ denotes the membrane tension, $K$ is the membrane wavenumber, $p_{inc}$ is the incident acoustic pressure, and $p(r)$ represents the $r-$dependent acoustic pressure behind the membrane. The solution to equation (4) is searched for in the form of an eigenfunction expansion

$$\xi(r) = \sum_n \xi_n \Psi_n(r), \tag{5}$$

where the eigenfunctions $\Psi_n(r)$ are given by

$$\Psi_n(r) = \frac{1}{\sqrt{\pi} R J_1(K_n R)} J_0(K_n r), \tag{6}$$

with $K_n$ determined by the membrane boundary conditions $\xi(R) = 0$. The modal coefficients $\xi_n$ are expressed as

$$\xi_n = \frac{1}{T(K^2 - K_n^2)} \iint_S (p_{inc} - p(r)) \Psi_n \mathrm{d}S, \tag{7}$$

where $S = \pi R^2$ denotes the membrane surface area.

### 2.3 Acoustic pressure inside the transducer

The acoustic pressure behind the membrane comprises two parts

$$p(r) = \begin{cases} p_h = \text{const.} & \text{for } r \in (0, R_h), \\ p_g(r) & \text{for } r \in (R_h, R), \end{cases} \tag{8}$$

where $p_h$ is assumed to be constant over the cross-sectional area of the central hole $S_h = \pi R_h^2$. Following the approach in [9], the acoustic pressure in the air gap is governed by the wave equation

$$\Delta_r p_g(r) + \chi^2 p_g(r) = \zeta\, \xi(r), \tag{9}$$

where $\zeta$ is an auxiliary source term and $\chi$ is a complex wavenumber that accounts for thermoviscous losses, as described in [9]. The solution to equation (9) is sought in the form

$$p_g(r) = A J_0(\chi r) + B Y_0(\chi r) + \sum_n p_n \Psi_n(r), \tag{10}$$

where $A$ and $B$ are integration constants determined by the following boundary conditions: (i) zero acoustic velocity at $r = R$, (ii) continuity of the acoustic pressure at $r = R_h$, and (iii) continuity of the volume velocity at $r = R_h$.

### 2.4 Coupling between membrane displacement and acoustic pressure

Substituting the expression for the acoustic pressure $p(r)$ into equation (7), the modal coefficients are obtained as follows

$$\frac{T(K^2 - K_n^2)}{2\pi}\xi_n = b_n + \sum_{mn} \xi_m C_{mn}, \tag{11}$$

which can be rewritten in matrix form as

$$\{[\mathbb{U}] - [\mathbb{C}]\}(\Xi) = (B), \tag{12}$$

where $[\mathbb{C}]$ is the matrix composed of elements $C_{mn}$, and $[\mathbb{U}]$ is a diagonal matrix with elements $T(K^2 - K_n^2)/2\pi$. The vectors $(\Xi)$ and $(B)$ represent the modal coefficients $\xi_n$ and the excitation terms $b_n = p_{inc}\int_0^R \Psi_n(r) r \mathrm{d}r$, respectively.

### 2.5 Mean displacement and pressure sensitivity

The mean value of the membrane displacement over the active area of the fixed electrode $S_e$ is given by

$$\begin{aligned}\tilde{\xi} =& \frac{1}{S_e}\iint_{S_e} \xi(r)\mathrm{d}S_e = \\ =& \frac{2\pi}{S - S_h}\sum_n \xi_n \frac{RJ_1(K_nR) - R_hJ_1(K_nR_h)}{K_n\sqrt{\pi}RJ_1(K_nR)},\end{aligned} \tag{13}$$

where $S_e = S - S_h$.

Finally, the acoustic pressure sensitivity of the microphone is expressed as

$$\sigma = \frac{U_0}{p_{inc}}\frac{\tilde{\xi}}{h_g}. \tag{14}$$

### 2.6 Theoretical results

The results of the linear microphone model are presented in this section. The physical properties of air and the geometrical and material parameters of the microphone used in the theoretical calculations are summarized in Tables 1 and 2, respectively.

**Table 1**. Properties of the air

| Parameter | Value | Unit |
|---|---|---|
| Adiabatic sound speed $c_0$ | 343.2 | m/s |
| Air density $\rho_0$ | 1.2 | kg/m$^3$ |
| Shear dyn. viscosity $\mu$ | $1.8{\cdot}10^{-5}$ | Pa·s |
| Thermal conductivity $\lambda_h$ | $24{\cdot}10^{-3}$ | W/(m·K) |
| Specific heat at constant press. per unit of mass $C_p$ | 1005 | J/(kg·K) |
| Ratio of specific heats $\gamma$ | 1.4 | - |

**Table 2**. Dimensions of the system and material properties of the moving component

| Parameter | Value | Unit |
|---|---|---|
| Membrane radius $R$ | $18{\cdot}10^{-3}$ | m |
| Membrane thickness $h_m$ | $25{\cdot}10^{-6}$ | m |
| Air-gap thickness $h_g$ | $230\cdot10^{-6}$ | m |
| Radius of the hole $R_h$ | $0.8{\cdot}10^{-6}$ | m |
| Length of the hole $R_h$ | $1.6{\cdot}10^{-6}$ | m |
| Back cavity volume $V_c$ | $7.74{\cdot}10^{-6}$ | m$^3$ |
| Membrane density $\rho_m$ | 1944 | kg/m$^3$ |
| Membrane tension $T$ | 116.27 | N/m$^1$ |
| Polarization voltage $U_0$ | 165 | V |

The absolute value of the acoustic pressure sensitivity, expressed in decibels and computed using the linear analytical model described above, is shown in Figure 2 (blue curve). This analytical result is compared with a reference numerical model based on the finite element method (FEM), formulated according to [11] and implemented in the Comsol Multiphysics software (red dots). The comparison demonstrates good agreement between the two models when the first 10 modes are included in the analytical solution.

Using the calculated mean displacement (13), the nonlinear output voltage of the microphone (3) was computed, and the levels of the first three harmonic components were determined at each frequency. These frequency-dependent output levels, calculated for an incident acoustic pressure of $p_{inc} = 1$ Pa, are presented in Figure 3. A relatively large level difference between the harmonic components can be observed at this input pressure.

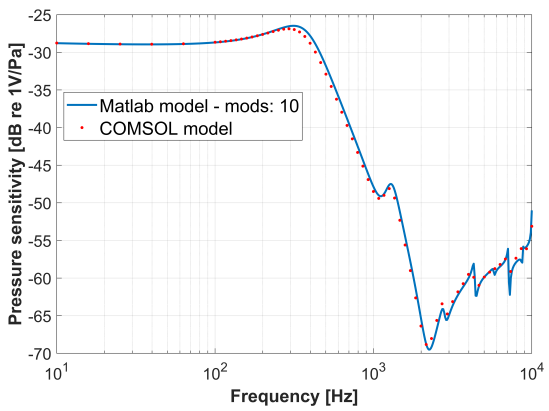


**Figure 2**. Comparison of the bsolute value of the acoustic pressure sensitivity in dB, calculated analytically (blue curve) and numerically using COMSOL Multiphysics (red dots).

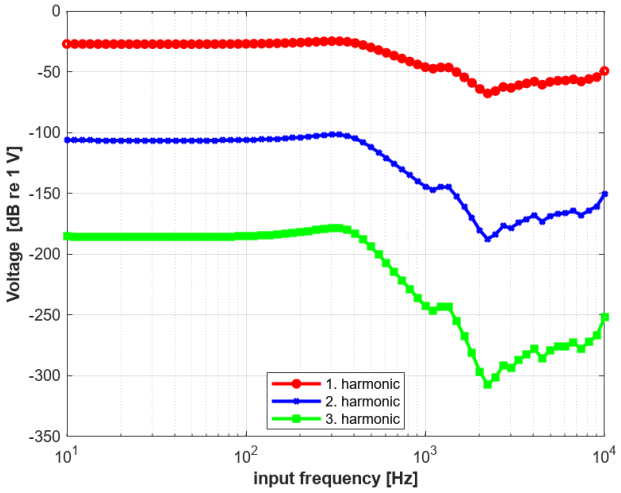


**Figure 3**. Absolute values of the harmonic components of the microphone output voltage in dB for $p_{inc} = 1$ Pa: 1st (fundamental) harmonic (red curve), 2nd harmonic (blue curve), and 3rd harmonic (green curve).

## 3. EXPERIMENTAL DEVICE AND MEASUREMENT SETUP

The experimental transducer (see Figure 4) consists of a circular membrane made of aluminum-metallized plastic foil, clamped at its periphery within a rigid 3D-printed frame. The fixed electrode, separated from the membrane by spacers forming the air gap, is fabricated from a printed circuit board (PCB) metallized with copper and coated with a thin gold layer on the side facing the membrane. The opposite side of the PCB hosts electronic components for signal amplification and power supply. A 3D-printed component forms the backing cavity and includes a threaded mechanism, which, when tightened, presses the PCB and spacers against the membrane, thus adjusting its tension. The dimensions of the system correspond to those listed in Table 2.

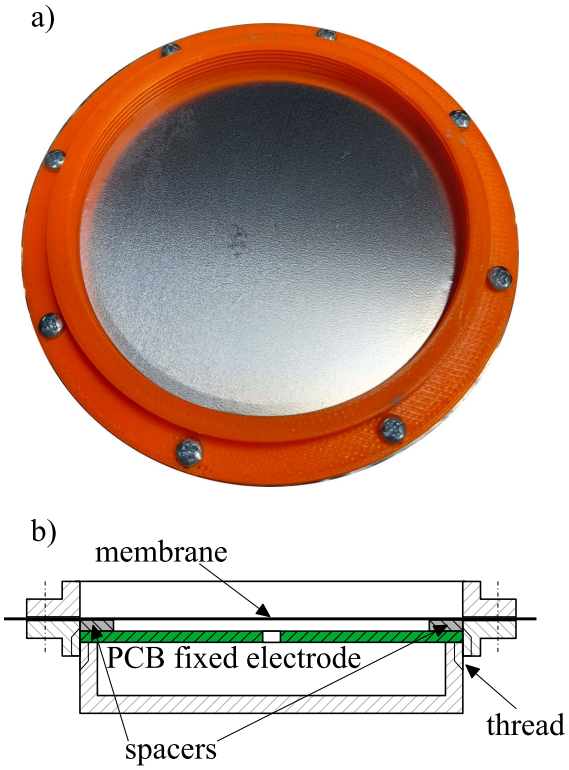


**Figure 4**. The experimental transducer: (a) top-view photograph; (b) schematic view of the assembly.

The measurement setup is shown in Figure 5. The experimental transducer, together with a reference microphone (B&K 4944-B, 3% THD at 170 dB SPL), is placed inside a measurement chamber between two loudspeakers (Visaton FR 12) arranged in a push-push configuration to generate high sound pressure levels with low distortion. The loudspeakers and both microphones are connected, via amplifiers, to a sound card (RME Fireface

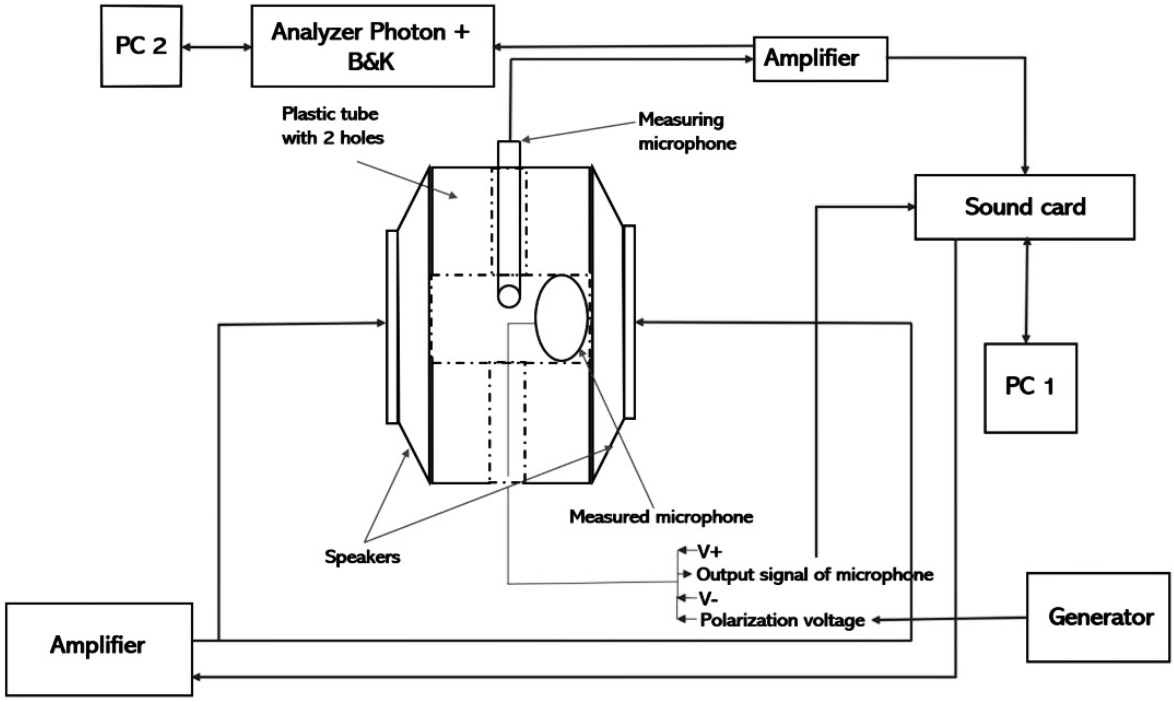


**Figure 5**. Schematic view of the measurement setup.

UCX), which is interfaced with computer PC1. Additionally, the output of the reference microphone is connected through an amplifier to a B&K Photon+ analyzer, which is linked to computer PC2 to monitor the exact sound pressure level inside the measurement chamber. To ensure purely harmonic excitation, a nonlinear harmonic correction technique was applied [7], effectively suppressing all undesired higher-order harmonics to the noise level. As a result, any nonlinearities observed in the output signal of the tested microphone originate solely from the microphone itself.

## 4. RESULTS

The measurement procedure described in the previous section was repeated for various levels of incident acoustic pressure and at different frequencies. For each measurement, the levels of the first three harmonics were extracted from the recorded output voltage of the tested microphone using a Fast Fourier Transform (FFT).

Figure 6 presents the results obtained at 110 Hz, which lies below the first resonance frequency of the transducer, for incident acoustic pressure levels ranging from 100 to 140 dB SPL. The points indicate the measured values for the first (blue points), second (orange points), and third (green points) harmonic components. The continuous lines represent the theoretical predictions based on the model described in the preceding sections. Similarly, Figure 7 shows results measured at 1 kHz, which is above the first resonance frequency of the transducer, for pressure levels between 90 and 130 dB SPL.

In both figures, the first and second harmonics are accurately predicted by the model. However, the third harmonic is observed to be between several decibels and approximately 40 dB higher than the levels predicted by the model. This discrepancy indicates that the third harmonic is influenced by additional sources of nonlinearity not accounted for in the analytical model, such as varying damping in the air gap with changing thickness or acoustic nonlinearities at high sound pressure levels within the gap.

## 5. CONCLUSION

An analytical model of an electroacoustic transducer with a circular membrane and a fixed electrode was developed, incorporating the coupling between membrane displace-

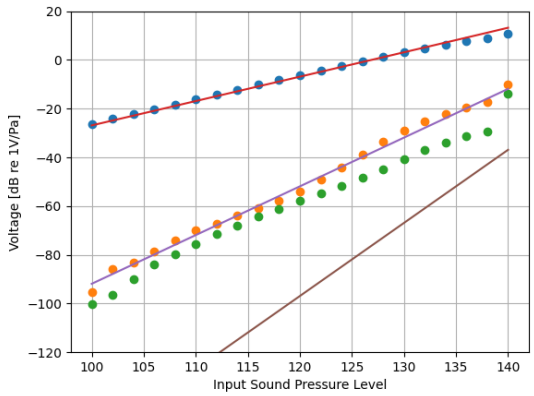


**Figure 6**. First three harmonic components of the microphone output voltage for different input sound pressure levels at 110 Hz.

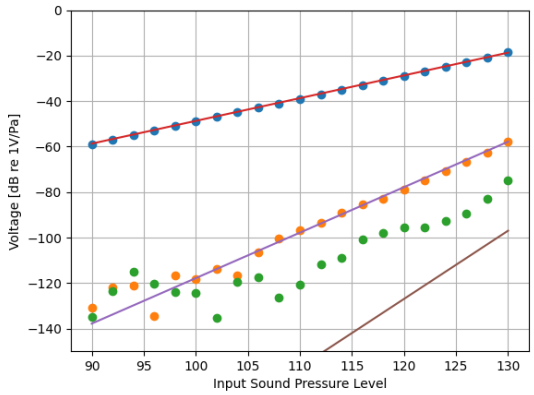


**Figure 7**. First three harmonic components of the microphone output voltage for different input sound pressure levels at 1 kHz.

ment and acoustic pressure in the air gap, as well as nonlinearities due to time-varying capacitance. The membrane response was expressed via eigenfunction expansion, leading to a formulation of the nonlinear output voltage. The model's predictions of acoustic pressure sensitivity were validated against numerical FEM results from COMSOL Multiphysics, showing good agreement when using the first ten modes.

An experimental transducer was built and measurements were carried out using harmonic excitation with nonlinear correction to isolate the transducer's intrinsic nonlinearities. The results confirmed that the model accurately predicts the first and second harmonic components. However, the third harmonic was significantly underestimated, indicating the presence of additional nonlinear effects, such as pressure-dependent damping or nonlinear acoustics in the air gap, not captured by the current model.

## 6. ACKNOWLEDGMENTS

This work was supported by grant No. SGS23/185/OHK3/3T/13 of the Czech Technical University in Prague.

## 7. REFERENCES

[1] A. Dessein, *Modelling distortion in condenser microphones*. PhD thesis, Technical University of Denmark, DTU, DK-2800 Kgs. Lyngby, Denmark, 2009.

[2] H. Pastillé, "Electrically manifested distortions of condenser microphones in audio frequency circuits," *J. Audio Eng. Soc.*, vol. 48, no. 6, pp. 559–563, 2000.

[3] E. Frederiksen, "System for measurement of microphone distortion and linearity at very high sound levels," *The Journal of the Acoustical Society of America*, vol. 110, pp. 2670–2670, 11 2001.

[4] A. Novak and P. Honzík, "Measurement of nonlinear distortion of mems microphones," *Applied Acoustics*, vol. 175, p. 107802, 2021.

[5] E. Frederiksen, "Reduction of non-linear distortion in condenser microphones by using negative load capacitance," in *Proceedings of InterNoise 96*, (Liverpool, UK), pp. 2679–2684, Institute of Noise Control Engineering, June 30–August 2 1996.

[6] P. Honzík and A. Novak, "Reduction of nonlinear distortion in condenser microphones using a simple post-processing technique," *The Journal of the Acoustical Society of America*, vol. 157, pp. 699–705, February 2025.

[7] A. Novak, P. Lotton, and L. Simon, "A simple predistortion technique for suppression of nonlinear effects in periodic signals generated by nonlinear transducers," *Journal of Sound and Vibration*, vol. 420, pp. 104–113, 2018.

[8] M. Bruneau, A.-M. Bruneau, Z. Škvor, and P. Lotton, "An equivalent network modelling the strong coupling between a vibrating membrane and a fluid film," *Acta Acustica*, vol. 1994, pp. 223–232, 06 1994.

[9] P. Honzík, A. Podkovskiy, S. Durand, N. Joly, and M. Bruneau, "Analytical and numerical modeling of an axisymmetrical electrostatic transducer with interior geometrical discontinuity," *The Journal of the Acoustical Society of America*, vol. 134, pp. 3573–3579, 11 2013.

[10] M. Bruneau and T. Scelo, *Fundamentals of Acoustics*. London: ISTE, 2006.

[11] N. Joly, "Finite element modeling of thermoviscous acoustics on adapted anisotropic meshes: Implementation of the particle velocity and temperature variation formulation," *Acta Acustica united with Acustica*, vol. 96, no. 1, pp. 102–114, 2010.